The Oslo Model and Self-Organised Criticality

February 17, 2019

Abstract

The Oslo model was inspired by the ricepile experiment, which is a common example for the concept of self-organised criticality. Through studying the behaviours of the height and the avalanche size, the self-organisation and criticality of the system was verified by the applications of finite size scaling and data collapse.

1 Introduction

The Oslo model was first proposed by Christensen *et al* (1996) to simulate the avalanche dynamics in the slowly driven ricepile experiment [1]. The model is driven by the addition of a single grain at the first site and the system responds to this perturbation by a series of avalanches (relaxations). The most distinct feature of the model is that the critical slopes of sites are selected randomly to be 1 or 2 in order to capture the real life spatial and temporal fluctuations. Despite the simplicity of the model, it displays self-organised criticailty such that the system spontaneous organised itself into the steady state and the probability of the avalanche size is scale invariant.
The objective of this project is to investigate the behaviours of the Oslo model by the measurements and analysis of the height and the avalanche size for different system sizes. The general framework for finite size scaling and data collapse was applied on the height and the avalanche size to examined whether the system demonstrates self-organised criticailty. The algorithn was implemented according to the instructions given in "Complexity Project Notes" [2].

2 Task 1

The Oslo model considers a system defined by two parameters: the lattice size L representing the number of sites, and the probability p for the threshold slope $z^{th} \in 1, 2$. The efficacy of the algorithm implemented was examined in order to ensure the results generated are valid.
The first test involves the analysis of two extreme cases where $p = 0$ and $p = 1$. This measure essentially reduces the Oslo model to the BTW models with fixed $z^{th} = 2$ and 1 respectively.
For the BTW model, it is expected that the height $h(t;L)$ over time should behave as a progressively flattened staircase. For each grain added to the first site, a series of avalanches methodically occur until all $z_i \leq z^{th}$. This process takes longer when more sites are filled up and more relaxations are required to bring the system to a stable transient configuration.
More specifically, the time required for the height to step up by one unit increases arithmetically until the system reaches its only recurrent configuration in steady state. The quantitative details for

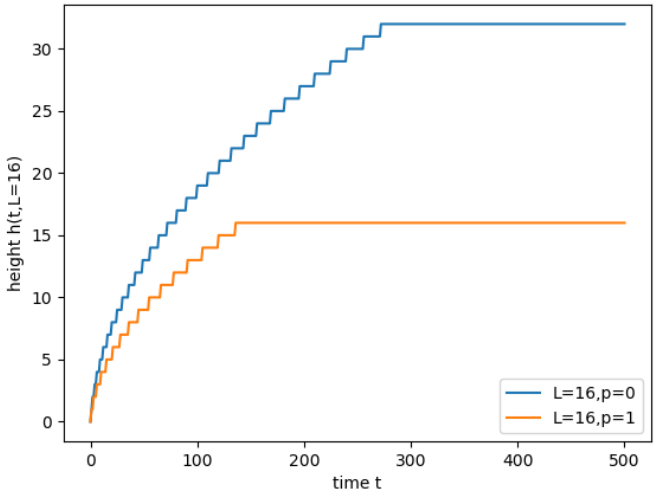

Figure 1: Plot of height $h(t;L)$ over time t for the system size $L = 16$ with probabilities $p = 0$ (blue line) and $p = 1$ (orange line)

$p = 0$ and $p = 1$ are provided in Table 1. For the case where $L = 16$ plotted in Figure 1, it can be observed that the behaviours of results agree perfectly with the predictions.

	z^{th}	$\langle h(t;L)\rangle$	t_c	$t_{h\to h+1}$
$p=0$	2	$2L$	$L(1+L)$	$(h\%2)+1$
$p=1$	1	L	$\frac{1}{2}L(1+L)$	$h+1$

Table 1: Two possible probabilities for the BTW model and their corresponding threshold slope, height in steady state, cross-over time, and time taken for a specific height to increase by one

The second test considers the average height in steady state $\langle h(t,L)\rangle_t$ given $p = 0.5$ for two system sizes $L = 16, 32$. The experimental $\langle h(t,L)\rangle_t$ values 26.52 ± 1.12 for $L = 16$ and 54.2 ± 1.35 for $L = 32$ were measured and compared against the known accepted ones 26.5 and 53.9. The results are both in good agreement with the predictions.
The examinations have verified that the Oslo algorithm was implemented successfully as intended and the data produced are correct and valid.

3 Task 2

This section involves measurements and analysis of the height of the pile $h(t;L)$ and and the cross-over time t_c with respect to different system sizes L. The simulation was iterated for 1.6×10^5 times for systems with $L = 4, 8, 16, 32, 64, 128, 256$. The first 10^5 iterations after t_c for each L were sampled to calculate the average time value $\langle h(t;L)\rangle_t$ for $h(t;L)$. The height of the pile $h(t;L)$ is defined as the height (number of grain) at the first site $i = 1$. Whereas the cross-over time $t_c(L)$ is the time when the first grain exit the system from the last site.

$$h(t;L) = \sum_{i=1}^{L} z_i(t) \tag{1}$$

$$t_c(L) = \sum_{i=1}^{L} z_i \cdot i \tag{2}$$

3.1 Task 2a

The heights $h(t;L)$ as functions of time t for various system sizes L were shown in Figure 2. It was observed that two distinct regimes were identified across all L. Over time, $h(t;L)$ increases at a decreasing rate until it passes a certain threshold and plateaus out. The disparate behavior signifies the abrupt transition from transient to recurrent configurations after t_c into the steady state, which is a characteristic time scale of the system.

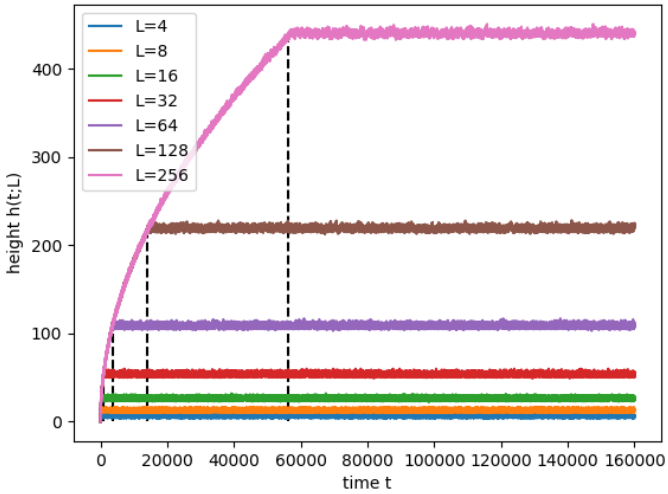

Figure 2: Plot of height $h(t;L)$ over time t for various system sizes $L = 4, 8, 16, 32, 64, 128, 256$. The black dashed lines represent the cross-over times t_c.

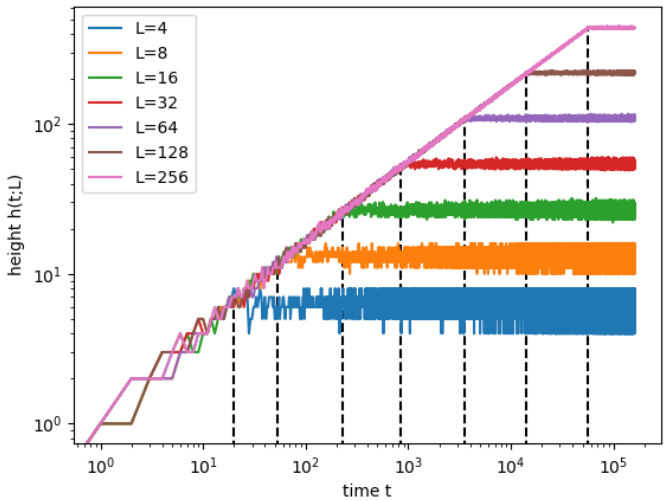

Figure 3: Plot of height $h(t;L)$ over time t for various system sizes $L = 4, 8, 16, 32, 64, 128, 256$ on log scale. The black dashed lines represent the cross-over times t_c.

On the log scale in Figure 3, it was revealed that $h(t;L)$ obeys some power law with respect to t ($h(t;L) \propto t_t^{\tau}$) in the transient state $t < t_c$. The exponent $\tau_t = 0.524 \pm 0.013$ was extracted through numerical analysis on the slope of the average steady state height (cross-over height) $h_c = \langle h(t > t_c) \rangle_t$ and t_c graph on log scale.

3.2 Task 2b

In contrast, the height in steady state with recurrent configurations $t > t_c$ fluctuates about an average value $\langle h(t;L) \rangle_t$, which increases with the system size L since Equation 1 can be rewritten as: $h(t;L) = \langle z_i \rangle L$. The experimental result in Figure 2 indicates that $h(t;L)$ in steady state has not time dependence, therefore the time average $\langle h(t;L) \rangle_t = \langle z_i \rangle L$ as well. As a result, the relation $\langle h(t;L) \rangle_t \propto L$ can be established becuase $\langle z_i \rangle$ tends to a constant value for $L \gg 1$,
Through exploiting the simulated data and calculating the slope on the log scale in Figure 4, the exponent obtained is 1.020 ± 0.004 for all data points. The disagreement in terms of the uncertainty range with the theoretical value 1 can be explained by the inclusion of the relatively small L. For the case where $L = 4, 8$ are eliminated, the exponent becomes 1.013 ± 0.003 and is more consistent with the theory.

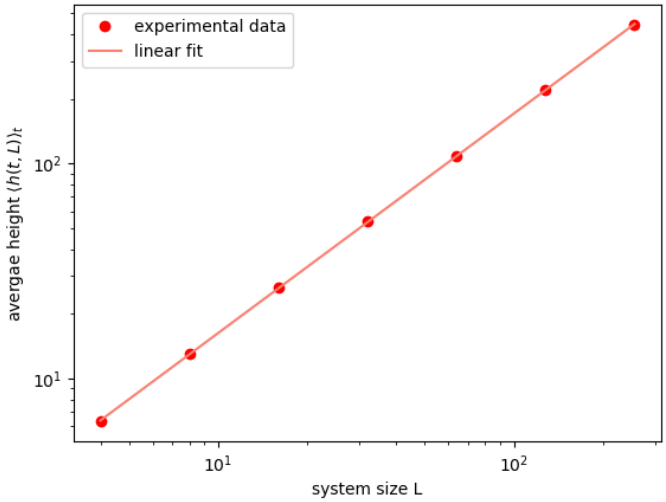

Figure 4: Plot of average height $\langle h(t;L) \rangle_t$ versus system size L (dots) with the linear fit of the data (line) on log scale

On the other hand, the relationship between the average cross-over time $\langle t_c \rangle$ and the system size L can be derived by considering the physical change when the system enters the steady state. The average number of grain in steady system is $\frac{hL}{2}$ so that the system is a shape similar to a downward staircase. On average, for the first grain to leave the system, $\frac{hL}{2}$ grain must be added beforehand. By replacing h with $\langle z_i \rangle L$, $\langle t_c \rangle$ can hence be written as $\frac{1}{2}\langle z_i \rangle L^2$. Data analysis on the experimental result shown in Figure 5 reveals that $\langle t_c \rangle$ and L conforms to a power law with the exponent value of 1.945 ± 0.047 when the theoretical value is 2. If $L = 4, 8$ are discarded, the exponent calculated becomes 1.999 ± 0.029 and the consistency was greatly improved.
In conclusion, $\langle h(t;L) \rangle_t$ scales linearly with L and $\langle t_c \rangle$ scales with L^2 for $L \gg 1$:

$$\langle h(t;L) \rangle_t \propto L$$
$$\langle t_c \rangle \propto L^2$$

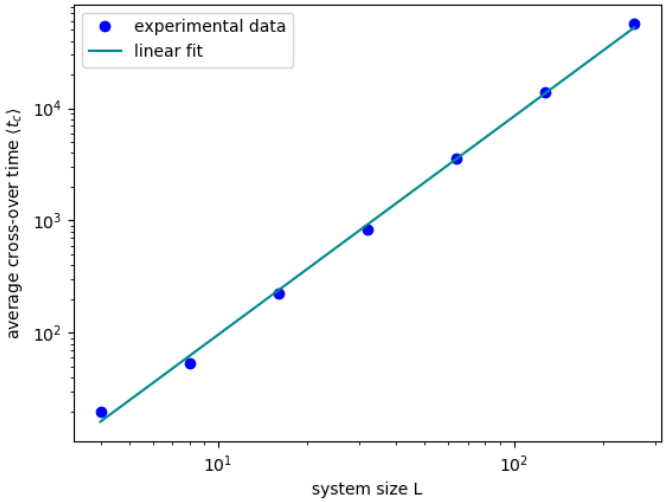

Figure 5: Plot of average cross-over time $\langle t_c \rangle$ versus system size L (dots) with the linear fit of the data (line) on log scale

3.3 Task 2c

Due to the inherited random nature of the model, smoothing the data via averaging can often facilitate the numerical analysis and improves the accuracy of the output. The average of height for M realisations $\tilde{h}(t;L)$ can be evaluated applying Equation 4:

$$\tilde{h}(t;L) = \frac{1}{M}\sum_{j=1}^{M} h^j(t;L) \tag{3}$$

where M is the number of realisations sampled and $h^j(t;L)$ is the height at time t for the system size L in the j^th realisation.
For this specific task, the simulation was iterated for 8×10^4 times as the process was very time-consuming. $\tilde{h}(t;L)$ for 100 realisations was evaluated and plotted against time in Figure 6.
Following the previous scaling arguments which were verified both theoretically and experimentally, the data collapse for different system sizes L can be performed by transforming the height to $\frac{\tilde{h}(t;L)}{L}$ and time to $\frac{t}{L^2}$. This result was plotted in Figure 7, which demonstrates that all systems sizes collapse onto the same graph of scaling function.
Mathematically, the relationship between the processed height $\tilde{h}(t;L)$ and the time t can be expressed as a scaling function $\mathcal{F}$ using the finite size scaling (FSS) ansatz:

$$\tilde{h}(t;L) \propto t_t^{\tau}\mathcal{F}(\frac{t}{t_c}) \tag{4}$$

because the cross-over time t_c is a characteristic time scale in this model. $\frac{t}{t_c}$ can be rewritten as $\frac{t}{L^2}$ since $t_c \propto L^2$ and $\tilde{h}$ is proportional to L in steady state so that

$$t_t^{\tau}\mathcal{F}(\frac{t}{L^2}) \propto L \quad \Rightarrow \quad \mathcal{F}(\frac{t}{L^2}) \propto (\frac{t}{L^2})^{-\tau_t} \propto L \tag{5}$$

For this to be true, τ_t has to be 0.5 so that $t^{0.5} \propto (L^2)^{0.5} \propto L$, and the final scaling function is

$$\tilde{h}(t;L) \quad \propto \quad t^{0.5}\mathcal{F}(\frac{t}{t_c}) \quad \propto \quad L\mathcal{F}(\frac{t}{L^2}) \tag{6}$$

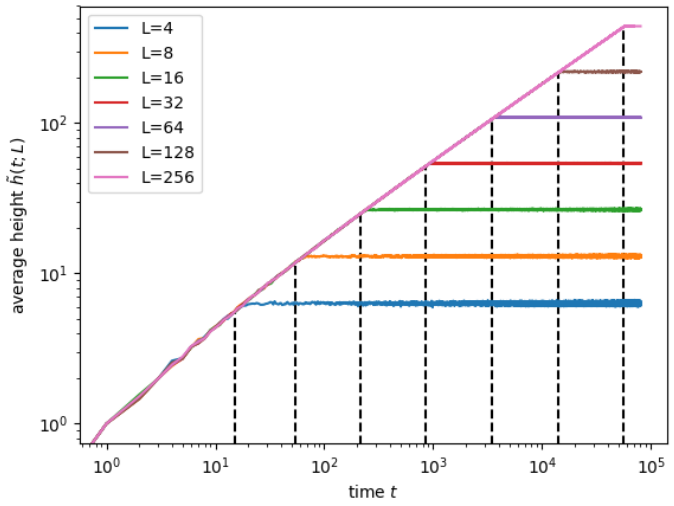

Figure 6: Plot of average height $\tilde{h}(t;L)$ over time t for various system sizes $L = 4, 8, 16, 32, 64, 128, 256$ over 100 realisations. The black dashed lines represent the cross-over times t_c.

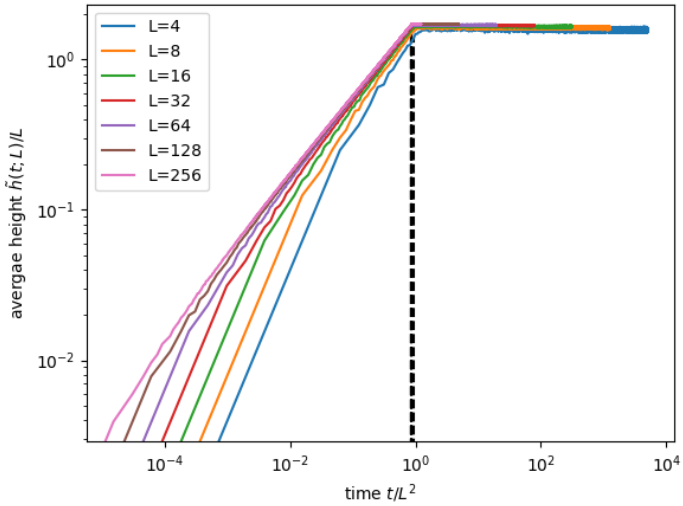

Figure 7: data collapse of average height $\tilde{h}(t;L)$ over time t for various system sizes $L = 4, 8, 16, 32, 64, 128, 256$ over 100 realisations on log scale. The black dashed lines represent the cross-over times t_c.

Let $x = \frac{t}{t_c}$. During the transient phase ($x \ll 1$), $\mathcal{F}$ simply equals 1 and this is consistent with the simulated result $\tau_t = 0.513 \pm 0.004$ obtained from linear fitting as the values differ by an acceptable percentage difference of 2.6%. Hence it can be said that $\tilde{h}$ increases with t according to a power law with an exponent of approximately 0.5. For recurrent state ($x \gg 1$), $\tilde{h}$ stays almost constant with small variations and can be considered as independent of t. $\mathcal{F}$ thus behaves as $\mathcal{F} \propto t^{-0.5}$ to counteract the exponential term.

3.3.1 Task 2d

The average slope for all sites $\langle z \rangle$ in Oslo algorithm is not simply 1.5 as one might naively guessed from the probability $p = 0.5$. Statistically, there exists more $z = 2$ than $z = 1$ because $z_{th} = 1$ is more likely to cause avalanches than $z_{th} = 2$. Consequently, there are more $z_{th} = 2$ as the system selectively update z_{th} to stabilise itself over time. As the result, $\langle z \rangle$ skewed towards 2 and it increases with L at a decreasing rate. Assuming that the behavior is homogeneous across all sites, sampling from one sites can be indicative for the system as a whole, thus $\langle z_i \rangle = \langle z \rangle$.
Applying this relation, $\langle t_c \rangle$ can be derived from Equation 2:

$$\langle t_c(L) \rangle = \sum_{i=1}^{L} \langle z_i \rangle \cdot i = \sum_{i=1}^{L} \langle z \rangle \cdot i = \frac{\langle z \rangle}{2} L^2 (1 + \frac{1}{L}) \tag{7}$$

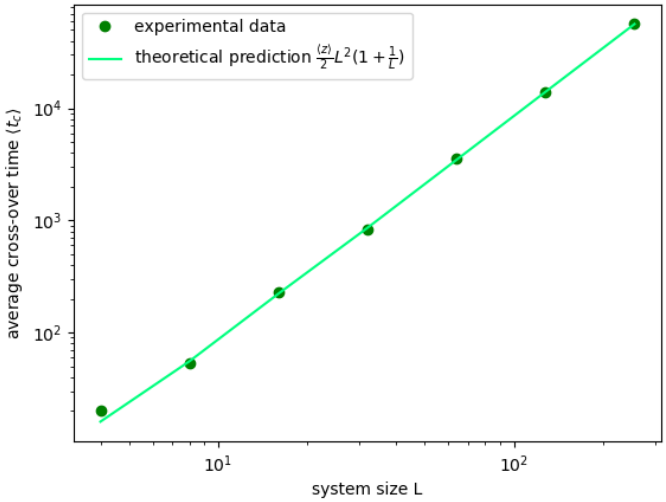

Figure 8: Plot of average cross-over time $\langle t_c \rangle$ versus system size L (dots) with the linear fit of the data (line) on log scale

From Figure 8, it can be visually observed that the data produced from simulation is consistent with the prediction and returns an acceptable mean difference of approximately 3.18%. The p-value of the fit is $0.570 \gg 0.050$ which further supports the hypothesis.

3.3.2 Task 2e

The scaling functions mentioned previously were derived under the premise that the system size $L \gg 1$, which is not strictly the case in this study as small systems $L = 4, 8$ were included in the analysis. From the disagreement in Task 2b regarding the experimental values of τ_h due to small L, it was determined that some higher degree corrections were required in order to get a more accurate expression of the general average height $\langle h(t;L) \rangle_t$:

$$\langle h(t;L) \rangle_t = a_0 L (1 - a_1 L^{-\omega_1} + a_2 L^{-\omega_1} + ...) \tag{8}$$

Where ω_i are positive exponents and a_i are constant.
For simplicity, a basic modification to up to $i = 1$ was implemented. A function with the form

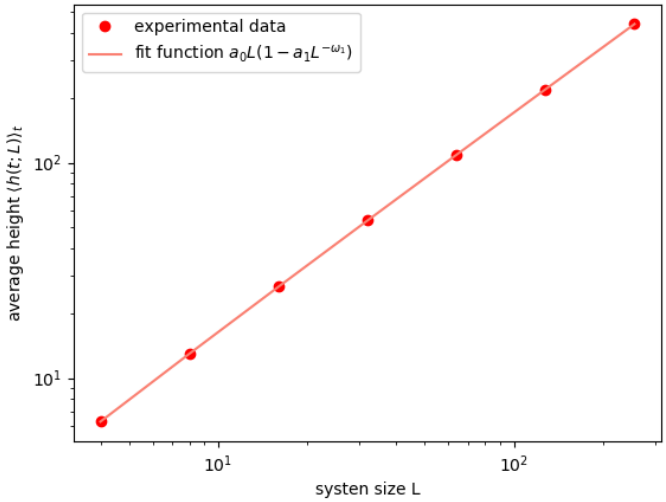

Figure 9: Plot of average cross-over time $\langle h(t;L)\rangle_t$ versus system size L (dots) with a fit function with the form $\langle h(t;L)\rangle_t = a_0L(1-a_1L^{-\omega_1})$ (line) on log scale

$\langle h(t;L)\rangle_t = a_0L(1-a_1L^{-\omega_1})$ was fitted to the data and the parameters were calculated computationally. The numerical values acquired were $a_0 = 1.737 \pm 0.001$, $a_1 = 0.207 \pm 0.007$, and $\omega_1 = 0.557 \pm 0.013$. It was found from Figure 9 that the fit is good with a small chi-squared value of 1.714×10^{-4} and a large p-value of approximately $1 \gg 0.05$. Equation 10 provides a sufficiently accurate expression for $\langle h(t;L)\rangle_t$:

$$\langle h(t;L)\rangle_t = 1.737L(1-0.207L^{-0.557}) \tag{9}$$

3.3.3 Task 2f

The correlation between the standard deviation of the height $\sigma_h(L)$ and the system size L is shown in Figure 10. It was deduced from the graph that it follows some power law. Assuming that no higher degree correction is needed and the function $\sigma_h(L)$ has a form of $b_oL^{w_0}$. From the fitting, the parameters were found to be $b_0 = 0.589 \pm 0.006$ and $w_0 = 0.237 \pm 0.002$. The fit also has a small chi-squared value of 5.458×10^{-4} and a great p-value of almost $1 \gg 0.05$ to verify the accuracy of the result therefore the correction with higher order term is not necessary.

$$\sigma_h = 0.589L^{0.237} \tag{10}$$

By revisiting the relation $\langle h(t;L)\rangle_t = \langle z\rangle L$ and error propagation, the average slope $\langle z\rangle$ and its standard deviation σ_z can be derived:

$$\langle z\rangle = \frac{\langle h(t;L)\rangle_t}{L} \propto 1.737(1-0.212L^{-0.560}) \tag{11}$$

$$\sigma_z = \frac{\sigma_h}{L} \propto 0.593L^{-0.765} \tag{12}$$

Therefore, for $L \to \infty$, $\langle z\rangle \to 1.737$ and $\sigma_z \to 0$.

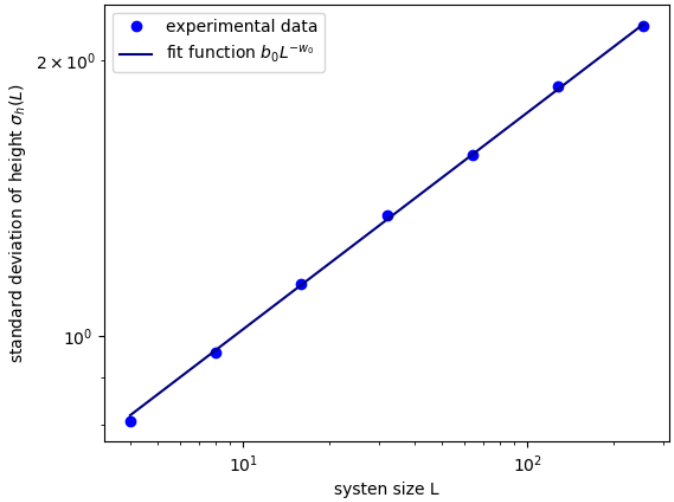

Figure 10: Plot of average cross-over time $\langle t_c \rangle$ versus system size L (dots) with a fit function with the form $\sigma_h(L) = b_o L^{w_0}$ (line) on log scale

3.3.4 Task 2g

The normalised height probability $P(h;L)$ for a system size L is defined as the number of configurations with height h divided by the total number of configurations. From the central limit theorem, it is expected that the probability distribution should behave as a Gaussian centred at the average height $\langle h(t;L) \rangle_t$ with a width of the standard deviation σ_h obtained from Task 2e, 2f for $L \gg 1$.

$$P(h;L) = \frac{1}{\sigma_h \sqrt{2\pi}} e^{-\frac{(h-\langle h \rangle)^2}{2\sigma_h^2}} \tag{13}$$

In Figure 11, each distribution approximately follows a Gaussian shape. the position of the peak of each distribution curve corresponding to $\langle h(t;L) \rangle_t$ conforms to the previous result that $\langle h(t;L) \rangle_t$ is directly proportional to L as the gap between consecutive peaks incrementally doubles.
Deriving from Equation 13, data collapse of $P(h;L)$ against h can be computed using the processed variables $\sigma_h P(h;L)$ and $\frac{h-\langle h \rangle}{\sigma_h}$. The probability distribution for data collapse can be rearranged as a new Gaussian with mean of 0 and standard deviation of 1:

$$\sigma_h P(h;L) = \frac{1}{\sqrt{2\pi}} e^{-\frac{u^2}{2}} \quad u = \frac{(h - \langle h \rangle)}{\sigma_h} \tag{14}$$

The outcome generated is shown in Figure 12. The fitted Gaussian $G(\mu = 0, \sigma = 1)$ generally agrees with the data collapse and the probability distribution behave very similar to a Gaussian. However, the slight deviations suggest that it does not completely match $G(\mu = 0, \sigma = 1)$ and the theoretical prediction. This can be explained by the false assumption that $\langle z_i \rangle$ is independent and random for the central limit theorem to be valid. In the model, the slopes of individual sites are not independent as they interact with their closest neighbours through relaxations. The slopes are also not unconditionally random because only the relaxed sites are selectively updated until the system stabilises. If this assumption were true, the central limit theorem and error propagation would suggest that $\sigma \propto L^{-0.5}$ since $\sigma_{\langle z_i \rangle} = \frac{\sigma_{z_i}}{\sqrt{L}}$ and $h = L\langle z_i \rangle$. This prediction is inconsistent with the result from Task 2f which generated an exponent of 0.237 ± 0.002, therefore it is likely that the application of the central limit theorem is invalid.

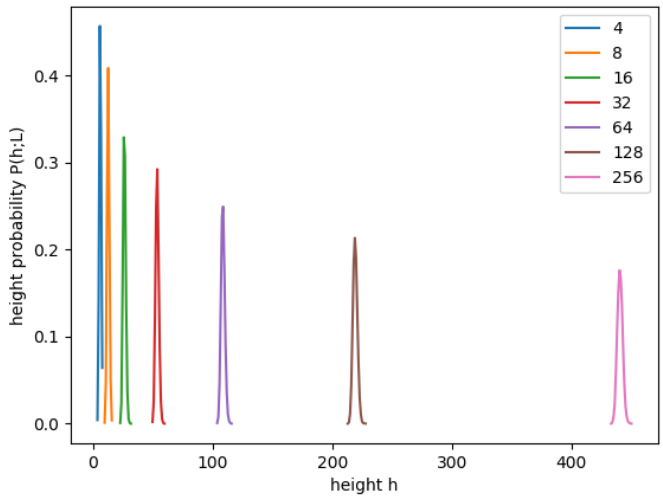

Figure 11: Plot of height probabilities $P(h;L)$ versus height h for various system sizes $L = 4, 8, 16, 32, 64, 128, 256$

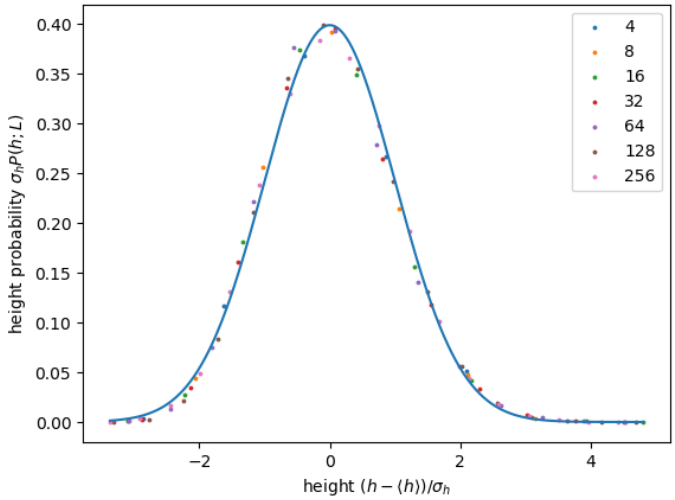

Figure 12: Plot of processed height probabilities $\sigma_h P(h;L)$ versus height $(h-\langle h\rangle)/\sigma_h$ for various system sizes $L = 4, 8, 16, 32, 64, 128, 256$ (dots) and a Gaussian distribution with $\mu = 0$ and $\sigma = 1$ (blue line)

4 Task 3

This section involves measurements and analysis of the avalanche size s with respect to different system sizes $L = 4, 8, 16, 32, 64, 128, 256$. The simulation was iterated for 1.6×10^5 times and the first 10^5 iterations after the cross-over time t_c for each L were sampled to calculate the average avalanche size $\langle s^k \rangle$ for a given k value.
The avalanche size s is defined as the number of consequent relaxations driven by the addition of one grain at site $i = 1$. The corresponding normalised avalanche size probability $\tilde{P}(s;L)$ is measured by the number of avalanches of size s relative to the total number of avalanches for a specific system size L.

4.1 Task 3a

The log-binning process was performed on the 10^5 samples of the avalanche size s for individual systems with the size L using a scale parameter of 1.5. The log-binned data was generated from the function '$logbin()$' in the file "logbin6-2-2018.py", and the result was plotted in Figure 13.

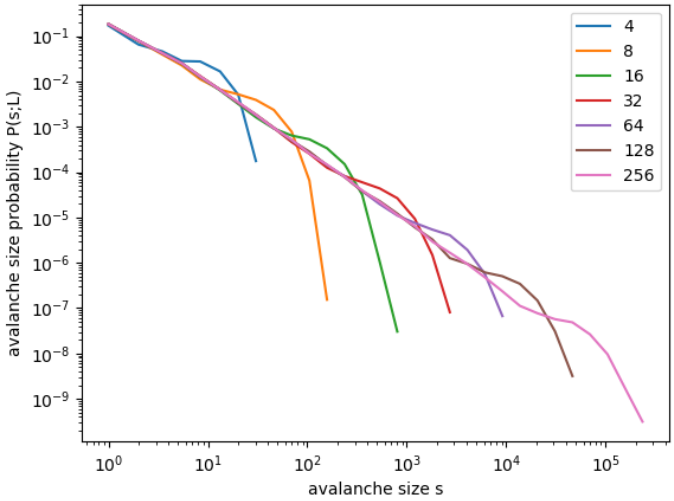

Figure 13: Plot of avalanche size probabilities $\tilde{P}(s;L)$ versus avalanche size s for various system sizes $L = 4, 8, 16, 32, 64, 128, 256$ on log scale

From the graph, it can be observed that some general features are universal across all L. For example, the avalanche size probability $\tilde{P}(s;L)$ obeys a power law with respect to s initially for all L. Conversely, as s becomes larger, $\tilde{P}(s;L)$ eventually reaches a cutoff avalanche size $s_c(L)$ that depends on L and decreases rapidly after a pronounced bump. In other words, $\tilde{P}(s;L)$ is scale invariant and decays according to a power law with s for $s_c(L) \gg s \gg 1$. In contrast, $s_c(L)$ scales with some power law of L as indicated by the incremental increase of $s_c(L)$ for greater L on log scale. In summary, the qualitative analysis on $\tilde{P}(s;L)$ suggests:

$$\tilde{P}(s;L) \propto s^{-\tau_s} \tag{15}$$

$$s_c(L) \propto L^D \tag{16}$$

4.2 Task 3b

Following the analysis on the avalanche size s in Task 3a, it was hypothesised that the avalanche size probability $\tilde{P}(s;L)$ conforms to the finite size scaling (FSS) ansatz for $L \gg 1$, $s \gg 1$:

$$\tilde{P}_N(s;L) \propto s^{-\tau_s} \mathcal{G}\left(\frac{s}{s_c(L)}\right) \tag{17}$$

where τ_s is the avalanche size exponent, D is the avalanche dimension, and the cutoff avalanche size $s_c(L) \propto L^D$ is the characteristic length scale. To investigate if the hypothesis is consistent with the data, Equation 16 was rearranged to the form:

$$s^{\tau_s} \tilde{P}_N(s;L) \propto \mathcal{G}\left(\frac{s}{L^D}\right) \tag{18}$$

The numerical values of τ_s and D that produces the best vertical and horizontal alignments respectively for the distinctive bumps were evaluated by data collapse. As the result, the estimated values determined are $\tau_s = 1.53 \pm 0.03$ and $D = 2.15 \pm 0.03$. The result of data collapse was plotted in Figure 14.

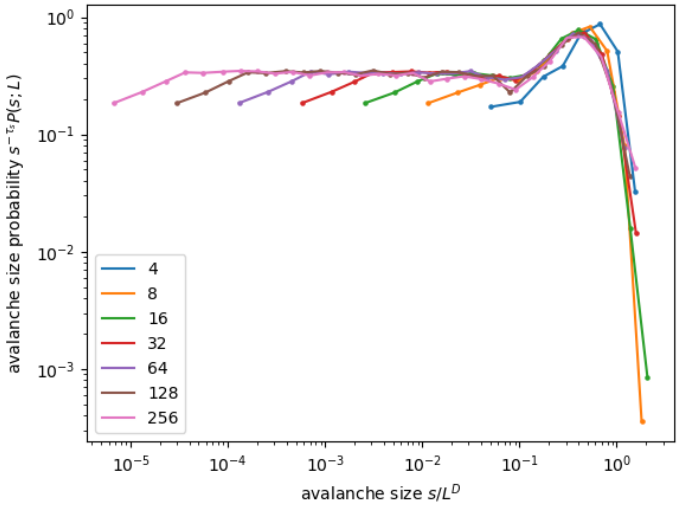

Figure 14: Plot of processed avalanche size probabilities $s^{\tau_s}\tilde{P}(s;L)$ versus avalanche size s/L^D for various system sizes $L = 4, 8, 16, 32, 64, 128, 256$ on log scale. $\tau_s = 1.53$ and $D = 2.15$.

In steady state, the average number of grains entering the system is equal to the average number of grains leaving. In other words, there is on average a grain toppling over all sites and exiting the system for each addition of grain. Mathematically, it implies the average avalanche size $\langle s \rangle$ should scale with L: $\langle s \rangle \propto L$. Consequently, from $\langle s \rangle \propto L^{D(2-\tau_s)}$ (see Task 3c for derivation), the exponent is predicted to be $D(2-\tau_s) = 1$.
Substituting in the acquired values for τ_s and D gives the experimental value $D(2-\tau_s) = 1.011 \pm 0.066 \approx 1$, which agrees with the predicted value and further validates the hypothesis.

4.3 Task 3c

Assuming the FSS ansatz for $\tilde{P}(s;L)$ holds for all avalanche size s, and the sum over s can be approximated as an integral, the k^{th} avalanche size moment $\langle s^k \rangle$ can be expressed as:

$$\langle s^k \rangle = \sum_{s=1}^{\infty} s^k \tilde{P}_N(s;L) = \sum_{s=1}^{\infty} s^{k-\tau_s} \mathcal{G}(\frac{s}{L^D}) \tag{19}$$

$$\propto \int_1^{\infty} s^{k-\tau_s} \mathcal{G}(\frac{s}{L^D}) ds \tag{20}$$

$$\propto \int_{1/L^D}^{\infty} (L^D u)^{k-\tau_t} \mathcal{G}(u) L^D du \tag{21}$$

$$\propto L^{D(1+k-\tau_s)} \int_{1/L^D}^{\infty} u^{k-\tau_s} \mathcal{G}(u) du \tag{22}$$

The integral part can be reduced to a constant as it converges at both upper and lower limits. Figure 13 shows that the scaling function $\mathcal{G}(u)$ decays rapidly at upper limit so that the integral converges.

On the other hand, for lower limit, the integral also converges given that $k - \tau_s > -1$ [3]. As a result, the $\langle s^k \rangle$ scales with the system size L for $L \gg 1$ according to:

$$\langle s^k \rangle \propto L^{D(1+k-\tau_s)} \tag{23}$$

For $k = 1, 2, 3, 4$, the simulated result for $\langle s^k \rangle$ with L is displayed in Figure 15. The plot clearly shows that $\langle s^k \rangle$ follows a power law relation with L where the exponent increases with k, as the theory suggested.

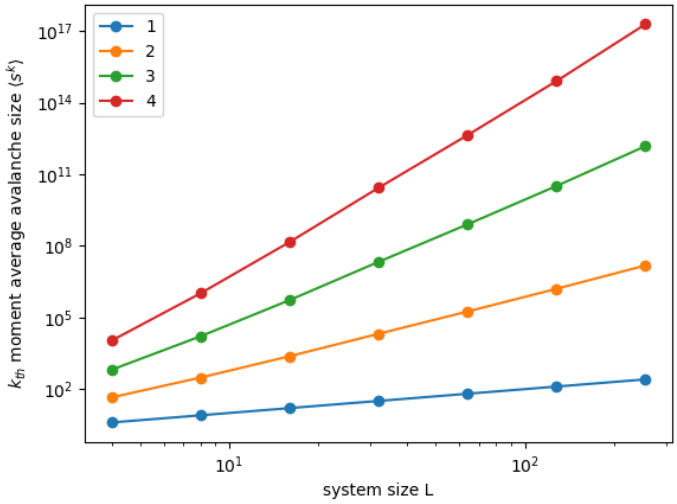

Figure 15: Plot of the k^{th} moment avalanche size $\langle s^k \rangle$ versus system size L for $k = 1, 2, 3, 4$ on log scale

In order to extract the values for τ_t and D, the slopes for individual k on log scales were calculated to find the values for $D(1+k-\tau_s)$. By plotting the $D(1+k-\tau_s)$ against k graph shown in Figure 16, the numerical values of τ_t and D were evaluated as the parameters in curve fitting.

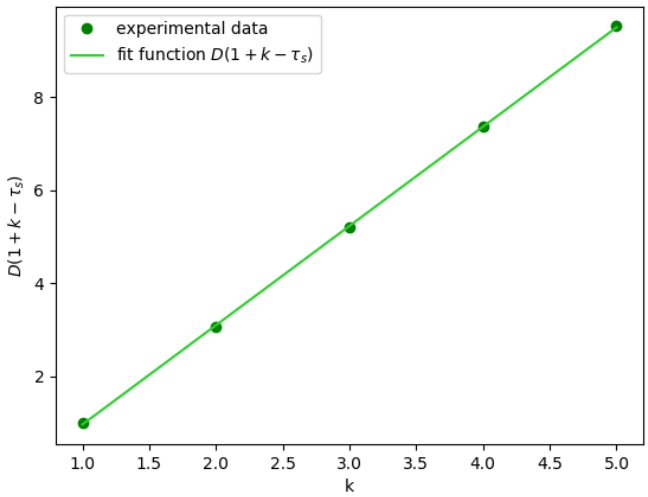

Figure 16: Plot of $D(1+k-\tau_s)$ versus k (dots) with a fit function (line) on log scale

The analysis returns the estimates $\tau_s = 1.539 \pm 0.014$ and $D = 2.121 \pm 0.013$. Repeating the same

test for $k = 1$ discussed in Task 3b, $D(2-\tau_s) = 0.978 \pm 0.036$ and it again confirms the result is consistent with the prediction. For τ_s, the experimental data agrees with the accepted value $\tau_s = 1.55$ with a small difference of 0.71%. However, the obtained D deviates from the accepted value $D = 2.25$ by a non-negligible 5.73% difference. This could be explained by the insufficiently large L considered in the analysis, hence some correction might be needed for the FSS ansatz for $\tilde{P}(s;L)$ to accommodate with small L.

5 Conclusion

The comprehensive analysis of the height and the avalanche size using the framework for finite size scaling and data collapse has confirmed that the Oslo model displays self-organised criticality. More accurate quantitative results can potentially be obtained by collecting data for larger system sizes. In order to achieve that, more efficient programming or more powerful hardware will need to be devised.

References

[1] V. Frette, K. Christensen, A. Malthe-SÃÿrenssen, J. Feder, T. JÃÿssang and P. Meakin, "Avalanche dynamics in a pile of rice", Nature, vol. 379, no. 6560, pp. 49-52, 1996. Available: 10.1038/379049a0.

[2] K. Christensen, "Complexity Project Notes", Imperial College London, 2019.

[3] K. Christensen and N. Moloney, Complexity and criticality. London: Imperial College Press, 2005.